REGISTRATION OF SAR AND OPTICAL IMAGES CONTAINING BRIDGES OVER LAND

Jan Dirk Wegner[1] *and Uwe Soergel*[1]

1. Leibniz University of Hannover, Institute of Photogrammetry and GeoInformation (IPI), Hannover, Germany; wegner@ipi.uni-hannover.de

ABSTRACT

Due to the very high resolution of state-of-the-art SAR sensors, both airborne (e.g. ESAR, PAMIR, MEMPHIS) and space borne (e.g. TerraSAR-X, CosmoSkyMed), new application scenarios arise especially in urban scenes. The focus of this paper is on bridges since they play a key role in urban infrastructure. Their condition has to be monitored and evaluated in particular in the case of natural hazards or political crisis. SAR scenes of bridges over water have already been examined. In this paper the appearance of bridges over land is discussed and some first findings of a long term project are presented. Due to layover effects and occlusion the interpretability of SAR imagery is deteriorated. One possibility to overcome such effects is the fusion of the SAR image with an optical image. The latter are basis of land surveying in many countries and it is reasonable to assume availability of such imagery in the archieves for comparison with actual SAR data. The optical image provides additional information in occluded areas as well as multi-spectral information. A semi-automatic registration approach based on line features is proposed for the improvement of the bridge scene of interest. In case of the optical image, a road extraction approach based on measuring spectral angels in colour imagery is used. Thresholding and morphological operators are applied for bridge extraction in the SAR image. In order to transform discrete line segments to continuous 2-dimensional information, distance maps are calculated. Such distance maps are then registered using a global transformation and a metric based on cross-correlation.

INTRODUCTION

Modern airborne SAR sensors provide geometric resolution well below half a meter. By means of SAR Interferometry (InSAR) from pairs of such images, a DEM of almost the same grid size can be obtained. Both, in single SAR images and in InSAR data, many features of urban objects become visible in detail, e.g. pillars of bridges. The characteristics of bridges over water in SAR imagery have already been discussed in detail for instance in (i,ii). In this paper high resolution SAR scenes containing bridges over land are introduced. They are somewhat more difficult to interpret because they do not show the multiple bounce line structure typical for bridges over water under certain viewing conditions. Their appearance very much depends on the terrain surrounding the bridge and on its superstructure. Additionally, the bridge height is important because the characteristic shadow of a bridge over land can only be seen clearly if the bridge is very high. A first step of analyzing and interpreting the new bridge scenes is to register them onto optical imagery. A simple semi-automatic registration approach was chosen in order to quickly register the images with reasonably good accuracy. In general, SAR/optical registration approaches are either pixel-based or feature-based. Pixel-based approaches tend to fail on above ground structures in high-resolution SAR/optical imagery due to significant geometric and radiometric differences. Therefore, pixel-based approaches show insufficient fusion accuracy particularly in urban scenes. Hence, an approach on a higher semantic level is required. Feature-based approaches have shown to deal well with geometric and radiometric differences and to provide appropriate fusion accuracy (iii,iv,v). The developed strategy is tested on aerial images with sub metric ground resolution. The single-pass X-Band InSAR data set (Figure 1(b)) has a resolution of approximately 38 cm in range and 18 cm in azimuth. It was acquired by Intermap Technologies with the AeS sensor. An optical image showing the same scene was taken by an aerial sensor (Figure 1(a)). Figure 2(c)) illustrates a fusion

ISBN 978-3-925143-79-3

result, which was achieved by extraction of the height information and true position from the SAR data and the bridge's width from the photo (1).The SAR images showing bridges over land (Figures 2(b) and 3) were captured with the MEMPHIS sensor by the Research Institute for High Frequency Physics and Radar Techniques (FHR) of the Research Establishment for Applied Science of the German Armed Forces (FGAN). Since corresponding aerial imagery for the scene of interest was not available, a screenshot from GoogleEarth (Figure 2(a)) was used here.

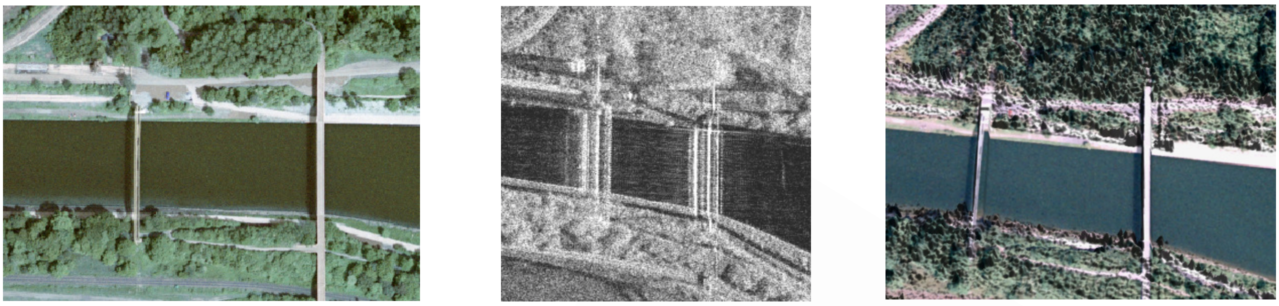

(a) (b) (c)

Figure 1: Test images of bridges near the city of Dorsten in southern Germany, (a) Optical aerial image, (b) InSAR magnitude image pair taken in X-Band (illumination direction from right to left), (c) 3D visualization of optical and InSAR data after fusion

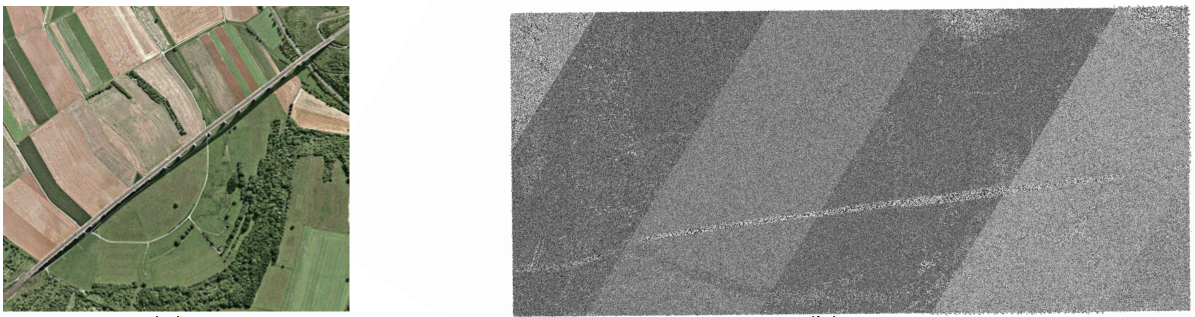

(a) (b)

Figure 2: Test images of a railroad bridge made of concrete-steel near the city of Zellingen in southern Germany, (a) Optical image from GoogleEarth, (b) SAR image taken by the MEMPHIS sensor in X-Band (illumination direction from top to bottom)

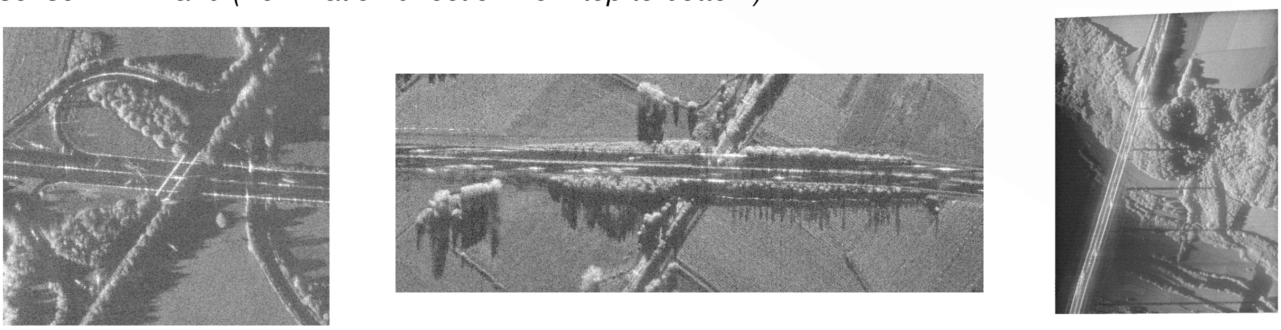

(a) (b) (c)

Figure 3: SAR test images of highway bridges acquired by the MEMPHIS sensor in X-Band, (a) SAR image of a bridge near Manching (illumination direction from left to right), (b) SAR image of a bridge near Wolnzach (illumination direction from top to bottom), (c) SAR image of a bridge near Schwaebisch Hall (illumination direction from left to right)

INSAR AND SAR IMAGERY OF BRIDGES

By comparing the InSAR (Figure 1(b)) and the SAR data set (Figures 2(b) and 3) it can clearly be seen that the appearance of bridges in SAR data strongly depends on their environment. The InSAR scene shows bridges over a calm water surface. Due to the very calm water and the perpendicular illumination direction, multiple-bounce effects occur. Hence, three parallel bright structures appear for each bridge. The first line in range direction corresponds to the layover of the direct bridge signal and the water signal. However, the direct signal from the bridge is dominant since most of the signal from the water surface is scattered away. Hence, this first stripe represents the height of the bridge body itself. The second line in range direction is due to double-bounce reflection between the bridge and the water surface directly under the bridge. Finally, the third one occurs due to a triple-bounce effect where the signal first hits the water surface, then the bottom side of the bridge and again the water surface. The slant range distance between the three stripes depends on the height of the bridge over the water surface. In order to calculate the bridges height, either the slant range distance Δs between the first and the second or the second and the third stripe have to be measured. Since we precisely know the off-nadir angle θ of the SAR sensor, the bridge height h can be determined: $h = \Delta s / \cos(\theta)$

In the SAR images covering scenes over land, the bridges appear differently. The double and triple-bounce effects that lead to two additional parallel lines in the InSAR data do not occur. This is due to the different reflectivity properties of soil and water. Calm water strongly reflects the signal whereas soil diffuses the signal. Hence, the bridge height cannot be measured directly from the line distances and the off-nadir angle. However, other features are worthwhile to be studied. The bridge body of the first test image (Figure 2(b)) appears particularly bright because of the rail-road track. Both the tracks and the power lines lead to strong backscatter. A large shadow area of the bridge over land occurs in the image. Since we can assume that the height of the bridge body and the flying altitude of the sensor are more or less constant, interesting measures can be conducted. For instance, the terrain height in the shadow area can be determined if the height of the bridge is known. The inverse way works as well. In case the terrain height in the shadow area is known, the height of the bridge can be estimated. The shadowed area may also be helpful for change detection purposes after the occurrence of natural hazards. The terrain height differences between the near range and the far range of the shadow of the bridge body can be determined if the width of the bridge body is known and vice versa. Additionally, the pillars of the bridge can be seen (Figure 4). The shadows of the bridge pillars may be observed, too. However, the upper parts of the pillars can probably not be seen because they are occluded by the bridge body. Therefore, it is difficult to estimate the bridge height by measuring the pillars' length in the image without additional information.

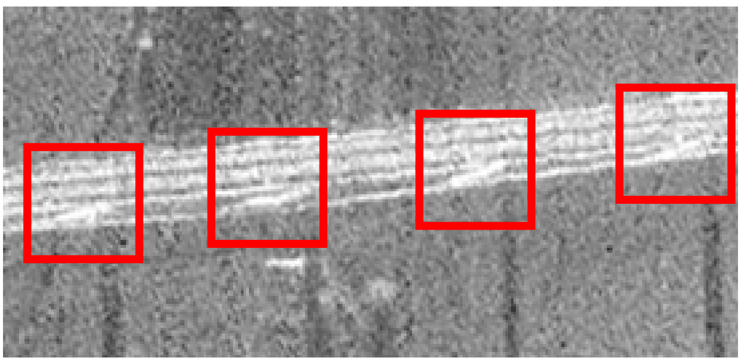

Figure 4: Bridge pillars (in red boxes) in the SAR image of the railroad bridge near Zellingen (illumination direction from top to bottom)

In Figure 4 details of different elements of the railroad bridge imaged by the SAR sensor are observable. Two relatively wide lines probably show the two railroad tracks on the bridge. Thinner lines display the superstructure of the bridge, e.g. the power lines of the railroad track.

The other three SAR test images shown in Figure 3 are more difficult to interpret. The highway bridges shown in the figures 3(a) and 3(b) are shorter and lower than the railroad bridge of Figure 2(b). Hence, the shadows of these bridges are not developed as nicely as in the railroad bridge case. Bright backscatter on the highway bridges occurs due to guardrails. Usually, one guardrail on each side of the bridge and one guardrail separating the lanes appears on highway bridges. These guardrails can be used for the estimation of the width of a bridge. In order to start with image analysis, first steps were limited to the SAR test image containing the railroad bridge shown in Figure 2(b). By comparing the SAR images of Figures 1, 2 and 3 it becomes obvious that detection of bridges over land in SAR imagery is a difficult task. The bridges' appearance strongly depends on the aspect, the bridge itself (height, superstructure) and the terrain surrounding it. Typical properties of bridges over land in SAR imagery are developed to their full extent in Figure 2(b). None-the-less, even in case of the railroad bridge, the outline is difficult to determine due to multiple-bounce and layover effects. Hence, a semi-automatic registration approach was applied to the test images (Figure 2(a) and 2(b)). An overview of this fusion approach is given in the following chapters.

FUSION STRATEGY OUTLINE

Different feature types may be thought of being useful for image registration, such as regions, points and lines. In urban areas, object boundaries of man-made objects consist mostly of straight contours. Therefore lines appear in high quantities. Hence, line features are extracted in both the SAR data and the optical image. For the optical image, a road extraction approach proposed in (vi) was applied. The SAR image is simply thresholded, since the rail road track is the brightest feature in the image. In order to transform lines to continuous 2-dimensional information, distance maps (Figure 5) are calculated from the line feature images.

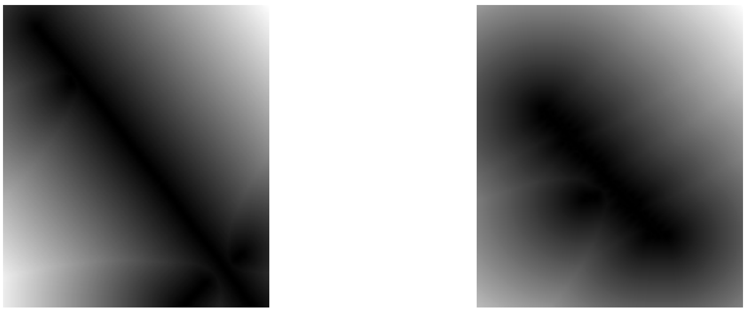

(a) (b)

Figure 5: (a) Distance map of the optical image, (b) Distance map of the SAR image

In order to register both optical and SAR images, a registration framework implemented in OTB(http://otb.cnes.fr) is used. As input to the registration framework, a master and a slave image have to be defined. In this case, the distance map derived from the threshold image of the SAR intensity image is considered the slave image. The distance map of the optical feature image is the master image, respectively. The slave image is then registered onto the master image by means of a similarity measure that calculates the cross-correlation of the images. After the SAR image has been registered onto the optical image, change detection can be conducted for instance in case of a natural hazard. We assume that the optical image was taken before and the SAR image immediately after the hazard. The goal is now to compare the condition of the bridge after the hazard with its condition before. A possible technique consists of comparing features that describe the vital parts of the bridge. This comparison can be conducted on pixel-level, feature-level and object-level.

ISBN 978-3-925143-79-3

FEATURE EXTRACTION AND IMAGE REGISTRATION

For our case of bridge detection the extraction of lines provides good results since we deal with long and narrow objects. Lines are directed features, too, which is an advantageous property concerning the rotation during registration. A robust road extraction approach presented in (6) is applied to the optical image. It calculates the spectral angle between the colour vectors in a multi-dimensional vector space which has the dimension of the number of spectral bands *b* (Figure 6(a)). The spectral angle, with a given reference pixel *r* and new pixels *p* to be assessed is defined as:

$$SA = \cos^{-1}\left(\sum_{b=1}^{n_b} r(b) \cdot p(b) / \sqrt{\sum_{b=1}^{n_b} r(b)^2 \sum_{b=1}^{n_b} p(b)^2} \right)$$

The more similar the reference pixel r and the new pixel p are, the smaller the spectral angle gets. Hence, all pixels belonging to roads will appear dark in the spectral angle image. Pixels showing almost no similarity with the reference pixel will lead to great spectral angles and thus will appear bright in the spectral angle image. A gradient filter is then applied to the spectral angle image. This gradient filter has two images as outcomes: a gradient intensity image and a gradient direction image. Since all roads are dark in the image, it can be assumed that the gradient directions on both sides of the road will be diametrically opposed. The scalar product of the gradient vectors in a neighbourhood with the radius one around the central pixel is calculated for each pixel of the gradient image. From the four pairs of pixels in the 3x3-neighbourhood the lowest negative scalar product is chosen. It points into the direction of the road. Pixels which do not show a maximum scalar product, i.e. the gradients are not exactly diametrically opposed, are removed. In the following, the road pieces are vectorized by transforming them to paths and vertices. Several steps are necessary in order to remove aligned paths, split paths if sharp angles occur (road curves are smooth in general) and to link paths that are almost aligned but show gap (due to e.g. tree shadows). Finally, a confidence value according to the spectral angle of the pixel is associated to the extracted road segments. In Figure 6(b) the extracted road segments are overlaid with the optical image.

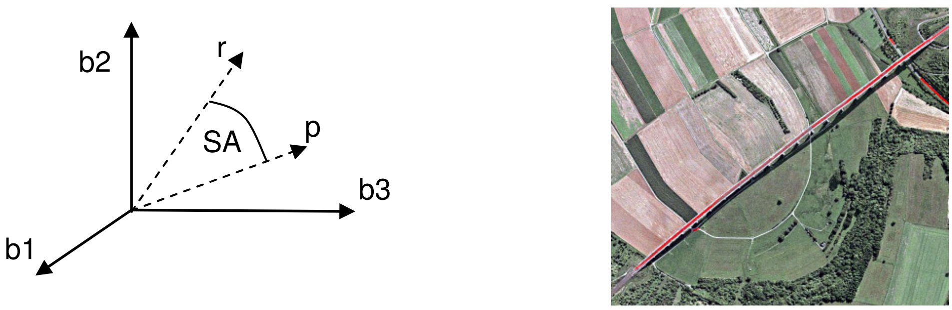

(a) (b)

Figure 6: (a) Multi-dimensional vector space with three bands b1 to b3, the vectors of the reference pixel r, the vector of the new pixel p and the spectral angle SA, (b) Optical aerial image of the railroad bridge overlaid with the extracted lines (red)

In the SAR image, the bridge body of the railroad bridge is extracted by applying a threshold. Since strong backscattering objects besides the bridge exist, morphological operations are carried out in order to optimize the result. Then, distance maps are calculated from the images containing the extracted bridges in order to transform the lines to continuous 2-dimensional information. Such distance images are then input to a registration framework (Figure 7) provided by OTB (vii). It registers a moving image onto a fixed with the indirect transformation method and consists of four components: a metric, an optimizer, a transform and an interpolator. For testing reasons, we choose a rather simple rigid transformation containing isotropic scaling, rotation and translation in x- and y-direction. For the interpolator a bi-linear approach is applied. The metric is a similarity measure which compares the moving with the fixed image. It was decided to use cross-correlation as the similarity measure. The entire registration process is driven by an optimizer that minimizes the metric value. The optimizer slightly changes the transform parameters after every iteration following the maximum gradient. Since we deal with rather small shifts, a gradient optimizer with a regular step size was applied.

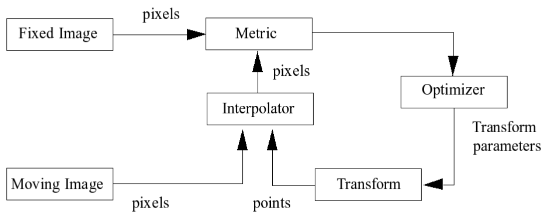

Figure 7: Sketch of the OTB registration framework

RESULTS

In order to allow for visual evaluation of the image registration, the results are displayed in a checker board scheme (Figure 8). The first checkerboard box in the upper left corner shows a part of the optical image. In the box on the right side of the first one a part of the SAR image is displayed. The following box again shows the optical image and so on. It can be seen that the images have been registered globally with good accuracy.

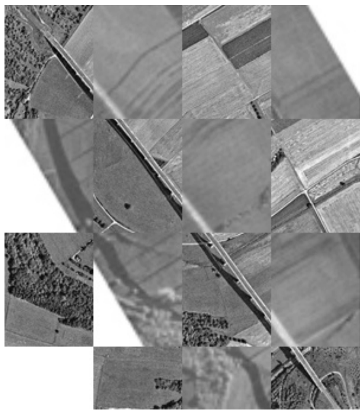

Figure 8: Checkerboard comparison of the SAR image and the optical after the registration

However, for fine registration further adjustments of the proposed registration approach are needed. Obviously, the bridges fit well onto each other but all other objects do not. This is due to the different viewing geometries of SAR (slant range) and optical (nadir) sensors. SAR images show layover, foreshortening and occluded areas because distances are measured from a side looking sensor. This is not the case for optical images where angles between objects are measured from a nadir perspective. The simple rigid transformation used during registration does not take into account such local displacements of elevated objects. Therefore, a non-rigid transformation is needed in order to further improve registration accuracy.

We also have to consider that we are dealing with a very particular case of image fusion. Since our object of interest is a railroad bridge, the railroad tracks appear very bright in the SAR image. Additionally, no other man-made structures leading to multiple-bounce effects and hence to strong backscattering of the signal exist in the image. Thus, it is relatively easy to properly extract the bridge body in this particular SAR image.

CONCLUSIONS

In this paper SAR scenes of bridges over water and bridges over land were compared. It was shown that scenes with bridges over land are difficult to interpret. However, they also show promising effects that can not be seen in case of bridges over water. Furthermore, an approach for the registration of SAR and optical imagery was presented. However, this approach only works properly if we make certain assumptions. First of all, the appearance of the bridge in the SAR image very much depends on the aspect. The test image shown in this paper (Figure 1(b)) was taken under perfect conditions, i.e. the SAR sensor was flying parallel to the bridge. Hence, all effects related to multiple bounces of the signal are very well developed. In addition, a shadow of the bridge pillars and the bridge body itself can be seen nicely in the image. This shadow therefore may be used for the bridge model since it distinguishes the bridge from a simple road or rail track. Furthermore, the shadow can be used for terrain height estimation and terrain modelling. Assuming we know the height of the bridge and the inclination of the sensor, we can estimate the terrain heights in the shadow area of the bridge body. In case we know the horizontal distance between the pillars' foundation and the shadow of the bridge body and additionally the terrain heights in the shadow area, we can estimate the height of the bridge.

In order to extract bridges over land in SAR images, more comprehensive modelling has to be carried out. For example, the bridge shadow of high bridges should be integrated in the bridge model in order to distinguish elevated bridges from flat roads. Additionally, a sophisticated line extraction approach as mentioned for example in (viii,ix,x) has to be integrated in order to detect the line features on top of the bridge body (railroad tracks, power lines, guardrails etc.). Finally, a object-based classification has to be conducted in order to properly detect bridges over land in SAR imagery.

Furthermore, a transformation taking into account the different viewing geometries of SAR and optical sensors has to be integrated. One possibility is to roughly register the images first with a rigid transformation that is then followed by a non-rigid registration for further refinements.

ACKNOWLEDGEMENTS

The authors thank FGAN-FHM for providing the SAR test images of the MEMPHIS sensor and Intermap fpr providing the InSAR data set. Thanks also go to our IPI colleagues Marcel Ziems and Sönke Müller for fruitful discussions.

REFERENCES

i Robalo J & J Lichtenegger, 1999. ERS-SAR Images a Bridge. ESA, Earth Observation Quarterly, 7 - 10

ii Soergel U, A Thiele, E Cadario, U Thoennessen, 2007. Fusion of High-Resolution InSAR Data and optical Imagery in Scenes with Bridges over water for 3D Visualization and Interpretation. In: Proceedings of Urban Remote Sensing Joint Event 2007 (URBAN2007), 6 p.

iii Dare P & I Dowman, 2000. A new Approach to Automatic Feature Based Registration of SAR and SPOT Images. International Archives of Photogrammetry and Remote Sensing, 33(B2): 125 - 130

iv Inglada J & F Adragna, 2001. Automatic Multi-Sensor Image Registration by Edge Matching using Genetic Algorithms. In: IEEE International Geoscience and Remote Sensing Symposium (IGARSS01), 5: 2313 - 2315 v Hong D H & R Schowengerdt, 2005. A Robust Technique for Precise Registration of Radar and Optical Satellite Images. Photogrammetric Engineering & Remote Sensing, 71(5): 585 - 593

vi Christophe E & J Inglada, 2007. Robust road extraction for high resolution satellite images. In: IEEE International Conference on Image Processing (ICIP07), 525 - 532

vii Inglada J, T Feuvrier, P Imbo, C Ruffel & Romain Garrigues, 2007. The ORFEO Tool Box Software Guide, Fifth Edition, Updated for OTB-2.0, chapter 8, 538 pp.

viii Tupin F, M Maître, J M Mangin, J M Nicolas & E Pechersky, 1998. Detection of Linear Features in SAR Images : Application to Road Network Extraction. IEEE Transactions on Geoscience and Remote Sensing, 36(2): 434 - 453

ix Wessel B, 2006. Automatische Extraktion von Straßen aus SAR-Bilddaten. PhD Thesis accomplished at the Technical University of Munich

x Hellwich O, 1997. Linienextraktion aus SAR-Daten mit einem Markoff-Zufalssfeld-Modell. PhD Thesis accomplished at the Technical University of Munich